

Identification and Characterization of Microvesicles Secreted by 3T3-L1 Adipocytes: Redox- and Hormone-Dependent Induction of Milk Fat Globule-Epidermal Growth Factor 8-Associated Microvesicles

Naohito Aoki, Shinji Jin-no, Yoshimi Nakagawa, Noriyuki Asai, Erina Arakawa, Noriko Tamura, Tomohiro Tamura, and Tsukasa Matsuda

Department of Applied Molecular Biosciences (N.Ao., S.J., T.M.), Graduate School of Bioagricultural Sciences, Nagoya University, Nagoya 464-8601, Japan; Department of Life Science (N.Ao., N.As., E.A.), Faculty of Bioresources, Mie University, Tsu 514-8507, Japan; Department of Internal Medicine (Y.N.), Institute of Clinical Medicine, University of Tsukuba, Tsukuba, Ibaraki 305-8575, Japan; Research Institute of Genome-Based Biofactory (N.T., T.T.), National Institute of Advanced Industrial Science and Technology, Sapporo 062-8517, Japan; and Laboratory of Molecular Environmental Microbiology (T.T.), Graduate School of Agriculture, Hokkaido University, Sapporo 060-8589, Japan

Adipocytes are now recognized as endocrine cells secreting adipocytokines, regulating multiple metabolic pathways. In this study, we addressed secretion of microvesicles by 3T3-L1 adipocytes. We found that MFG-E8, one of the exosomal proteins, was present in the microvesicles and was distributed in the sucrose density fractions with 1.13–1.20 g/ml, which has been reported for exosomes. Several integral, cytosolic, and nuclear proteins such as caveolin-1, c-Src kinase, and heat shock protein 70 were also found to be microvesicle components. Unexpectedly, adiponectin was also substantially distributed in the microvesicle fractions. Furthermore, proteomic analysis of the microvesicles revealed that many other proteins such as extracellular matrix-related proteins were also present. Microvesicles secreted by 3T3-L1 adipocytes exhibited heterogeneity in size and comprised both smaller exosome-like and larger membrane vesicles as revealed by electron microscopy.

Milk fat globule-epidermal growth factor 8 (MFG-E8)-associated adiposomes exhibited binding activity toward phosphatidylserine and apoptotic cells. MFG-E8 in the microvesicles was reduced when cultured in the low-glucose medium or cultured in the high-glucose medium with antioxidant *N*-acetyl cysteine. Insulin and TNF- α also up-regulated MFG-E8 in the microvesicles. Moreover, MFG-E8 was strongly up-regulated in the hypertrophic adipose tissue, predominantly in adipocyte fractions, of diet-induced obese C57BL/6 mice, where increased oxidative stress is induced. Thus, it is suggested that microvesicles, especially MFG-E8-associated ones, modulate adipose functions under redox- and hormone-dependent regulation. Based on the above findings, the adipocyte-derived microvesicles were named adiposomes. (*Endocrinology* 148: 3850–3862, 2007)

MEMBRANE VESICLES ORIGINATE from the plasma membrane via a mechanism morphologically similar to that of virus budding process. The vesicles are relatively large and heterogeneous in size ranging from approximately 100–1000 nm in diameter (1, 2). Vesicle shedding has been shown to be an active process that requires RNA and protein synthesis (3) and occurs in living cells showing no signs of apoptosis or necrosis. Vesicle membranes carry most of the cell surface antigens expressed on the plasma membrane of originating cells (4). However, these vesicles originate from do-

main of the plasma membrane selectively enriched in membrane components including histocompatibility leukocyte antigen class I molecules, β 1 integrin, and membrane-associated matrix metalloproteinase-9 (MMP-9) (5). Vesicle shedding has been associated with cell migration and tumor progression (6), which might be mediated by vesicle membrane-bound proteinases (5, 7–10). Such vesicles are also shed by several nontumor cells (11, 12) and have been reported to convey various regulatory factors (3, 4, 10, 13–16).

In addition to membrane vesicles, exosomes, a population of microvesicles released by living eukaryotic cells, have also been reported. Exosomes are 30- to 100-nm extracellular vesicles released by exocytosis of multivesicular bodies. These structures are part of the endosomal system and are considered to belong to late endosomes/lysosomes. Exosomes are probably generated by inward budding of the vesicle membrane (17, 18) and are enriched in major histocompatibility complex class I and II molecules, members of the tetraspanin protein family, heat shock protein 70 (HSP70), and milk fat globule-epidermal growth factor 8 (MFG-E8) (19–26). Two cytosolic proteins found in exosomes, galectin-3 and annexin II, are also found in the extracellular environment. Because

First Published Online May 3, 2007

Abbreviations: DAPI, 6-Diamidino-2-phenylindole; EF-1 α , elongation factor-1 α ; FCS, fetal calf serum; HF, high-fat; HSP70, heat shock protein 70; LF, low-fat; MFG-E8, milk fat globule membrane epidermal growth factor 8; MMP-9, matrix metalloproteinase-9; MS/MS, tandem mass spectrometry; NAC, *N*-acetyl cysteine; PAI-1, plasminogen activator inhibitor-1; PBST, PBS with 0.5% Tween 20; PS, phosphatidylserine; ROS, reactive oxygen species; SV, stromal vascular; TCA, trichloroacetic acid; TUNEL, terminal deoxynucleotidyl transferase-mediated deoxyuridine triphosphate nick-end labeling.

Endocrinology is published monthly by The Endocrine Society (<http://www.endo-society.org>), the foremost professional society serving the endocrine community.

these proteins do not possess a signal sequence, it has been suggested that exosomes represent an unconventional secretion pathway for these proteins (23).

We previously reported that COMMA-1D mammary epithelial cells secreted microvesicles associating with an exosomal component, MFG-E8 (27). MFG-E8 was originally characterized as 53- and 66-kDa proteins associated with the surface of the milk fat globule membrane. Recent reports uncovered that MFG-E8 was a missing link between apoptotic cells and phagocytes (28) and was indeed required for removal of apoptotic mammary epithelial cells in involuting mammary glands (29, 30). Furthermore, MFG-E8 has also been reported to promote vascular endothelial growth factor-dependent angiogenesis by using MFG-E8-deficient mice (31).

Adipocytes produce a variety of biologically active molecules collectively known as adipocytokines or adipokines (32, 33), including plasminogen activator inhibitor-1 (PAI-1), TNF- α , resistin, leptin, and adiponectin. Dysregulated production of these adipocytokines participates in the pathogenesis of obesity-associated metabolic syndrome. For instance, increased production of PAI-1 and TNF- α from accumulated fat contributes to the development of thrombosis (34) and insulin resistance (35, 36), respectively. In contrast, adiponectin exhibits insulin-sensitizing (37–40) and antiatherogenic effects (41–43), and hence a decrease in plasma adiponectin leads to insulin resistance and atherosclerosis. Thus, adipocytes are now recognized as endocrine cells, but it remains uncertain whether adipocytes produce microvesicles.

In the present study, we found that 3T3-L1 adipocytes secreted MFG-E8-associated microvesicles. They displayed a mixture of exosome-like and larger membrane vesicles by electron microscopy. Additional biochemical and proteomic analyses revealed that the microvesicles with exosomal features contained a variety of secreted, integral, cytosolic, and nuclear proteins. MFG-E8-associated adiposomes showed binding activity to phosphatidylserine (PS) and apoptotic Jurkat cells. Of note, MFG-E8 but not caveolin-1 in the microvesicles was greatly reduced when cultured in the low-glucose medium or cultured in the high-glucose medium supplemented with antioxidant *N*-acetyl cysteine (NAC). Insulin and TNF- α also up-regulated MFG-E8 in the microvesicles. In addition, MFG-E8 was strongly up-regulated in the epididymal adipose tissue of diet-induced obese mice, where increased oxidative stress was induced. MFG-E8 was shown to be expressed predominantly in the adipocyte fraction over the stromal vascular (SV) fraction of the adipose tissue. Thus, microvesicles, especially MFG-E8-associated ones, might modulate adipose functions under redox- and hormone-dependent regulation in hypertrophic adipose tissues.

Materials and Methods

Materials

Antibody to mouse MFG-E8 (44) was previously described. Antibody to human MFG-E8 was raised against the C-terminal half of the recombinant protein and will be described elsewhere (Ogura, A., N. Aoki, and T. Matsuda, unpublished data). Antibodies to c-Src (SRC2), caveolin-1 (N-20), HSP70 (W27), histone H2B (FL-126), and lamin B1 (M-20) were purchased from Santa Cruz Biotechnology Inc. (Santa Cruz, CA). Antibodies to caveolin-2 and flotillin-2 were from Transduction Laborato-

ries (Lexington, KY), and those to α -tubulin were from Oncogene Science Inc. (Manhasset, NY). Antibodies to adiponectin and resistin were kindly provided by Dr. Kihara (Osaka University) and Dr. Moriyama (Kinki University), respectively. AlexaFluor488-conjugated donkey anti-goat antibody and 6-diamidino-2-phenylindole (DAPI) were purchased from Invitrogen (Carlsbad, CA) and Nakarai Tesque (Kyoto, Japan), respectively. All other reagents were from Sigma or Wako Pure Chemicals (Osaka, Japan), unless otherwise noted.

Plasmids

cDNAs for adiponectin (U37222) and resistin (NM_022984) were amplified by PCR with Pyrobest *Taq* DNA polymerase (TaKaRa, Japan), inserted into pTarget vector (Promega, Madison, WI), and sequenced for confirmation.

Cell culture

3T3-L1 and NIH3T3 cells were maintained in DMEM (high-glucose, 4500 mg/liter; Sigma) supplemented with 10% fetal calf serum (FCS), which had been depleted of endogenous membrane vesicles by ultracentrifugation (45), unless otherwise noted. When confluence was reached (d 0), 3T3-L1 cells were incubated in a differentiation medium, which was the maintenance medium supplemented with 0.25 μ M dexamethasone, 10 μ g/ml insulin, and 0.5 mM 3-isobutyl-1-methylxanthine. After 48 h (d 2), the cell culture medium was changed to post-differentiation medium, which was the maintenance medium supplemented with 5 μ g/ml insulin, and then the medium was replaced with fresh medium every 2 d. Each conditioned medium was supplemented with 0.05% sodium azide and stored at 4 C until use. Rat adipocytes were prepared from epididymal adipose tissue of male Wistar KY rat by collagenase digestion and maintained in the same medium. Production of reactive oxygen species (ROS) was measured using nitroblue tetrazolium as described (46).

Cell lysis and Western blotting

Cells were lysed with lysis buffer containing 50 mM Tris-HCl (pH 7.5), 5 mM EDTA, 150 mM NaCl, 10 mM sodium phosphate, 10 mM sodium fluoride, 1% Triton X-100, 1 mM phenylmethylsulfonyl fluoride, and 10 μ g/ml leupeptin. Lysates were directly subjected to Western blotting with indicated antibodies. The protein bands were visualized with an enhanced chemiluminescence detection kit (Amersham Biosciences, Piscataway, NJ) and Light Capture system (AE-6962; ATTO, Tokyo, Japan).

Microvesicle preparation from conditioned media

Conditioned medium was first centrifuged at 1000 \times g for 5 min and then at 15,000 \times g for 15 min to remove cell debris and aggregates. The supernatant was ultracentrifuged at 100,000 \times g for 1 h. Pelleted vesicles were suspended in PBS and re-ultracentrifuged for washing. Pelleted vesicles were again resuspended in PBS and then subjected directly to Western blotting or subfractionation by flotation on sucrose density gradient. Pelleted vesicles were layered on a linear sucrose gradient (10–70% sucrose in PBS) prepared with Gradient Mate device (BIO-COMP, Frederickton, Canada) in a Beckman SW41 tube and was centrifuged at 200,000 \times g for 18 h. Gradient fractions of 900 μ l were collected from the top of the tube and subjected to trichloroacetic acid (TCA) precipitation, followed by SDS-PAGE and immunoblotting.

Ultrastructural analysis

Transmission electron microscopy of membrane vesicles was carried out using a standard technique. Briefly, cells were fixed with 2% glutaraldehyde/0.15 M sodium cacodylate in culture flasks, scraped, and postfixed with 1% OsO₄, dehydrated with ethanol, and embedded in Epon 812. Samples were sectioned, post-stained with uranyl acetate and lead citrate, and examined with an electron microscope (JEOL JEM2000EX, Tokyo, Japan). For immunoelectron microscopy, cells were fixed with 4% paraformaldehyde/2% glutaraldehyde/0.15 M sodium cacodylate and processed as above. Sections were probed with affinity-purified anti-MFG-E8 antibody or control rabbit IgG and visualized with ImmunoGold-labeled secondary antibody.

Proteomic analysis

Sample (30–40 μ g) was dried by centrifugation under vacuum and dissolved into 100 mM Tris-HCl (pH 8.5) containing 8 M urea and then reduced with 10 mM dithiothreitol at 37°C for 30 min and alkylated with 50 mM iodoacetamide in the dark for 1 h. To reduce urea concentration to 1 M, water was added to the sample, and then 1 μ g trypsin was added to digest the proteins at 37°C overnight. The resulting peptides were desalted by using of a MonoTip C18 (GL Sciences Inc., Tokyo, Japan) and eluted with 0.1% trifluoroacetic acid in 60% acetonitrile. Eluted peptides were dried and dissolved with 0.1% formic acid in 2% acetonitrile.

Tryptic peptides (~2 μ g) were separated by reverse-phase chromatography using a 0.2 mm inner diameter \times 75 cm NanoCap high-resolution 750 capillary column (GL Sciences) connected to a MAGIC 2002 liquid chromatography system (Michrom BioResources, Auburn, CA). Peptides were eluted during a 360-min linear gradient from 5–30% buffer B (buffer A contained 2% acetonitrile, 0.1% formic acid; buffer B contained 90% acetonitrile, 0.1% formic acid). The effluent from the liquid chromatography at a flow rate of 120 μ l/min was split by a MAGIC Splitter (Michrom BioResources) to approximately 1.0 μ l/min and directly introduced into an LCQ-DECA XP plus ion trap mass spectrometer (Thermo Electron, San Jose, CA) equipped with a nano-electrospray ion source (AMR Inc., Tokyo, Japan). Nano-electrospray ionization-tandem mass spectrometry (MS/MS) operation and data acquisition were carried out on an Xcalibur system (Thermo Electron).

All MS/MS spectra were searched against the NCBI mouse database and analyzed using the TurboSequest algorithm in the Bioworks 3.2 software package (Thermo Electron). The mass tolerance of the intact precursor and fragment ions was set at 2 and 1 Da, respectively. The MS/MS data files were searched allowing up to two internal missed tryptic cleavages. The following modifications were permitted: carbamidomethylated cysteine (+57 Da) and oxidized methionine (+16 Da). The identified peptides were further evaluated using the following filters: the numbers of top matches (=5), the ScoreFinal (Sf, ≥ 0.85) and the peptide probability ($\leq 1e-003$). ScoreFinal (Sf) combines five SEQUEST scores (Sp, RSp, Ions, XCorr, DeltaCn) using a neural network to reflect the strength of peptide assignment on a scale of 0.0–1.0; scores of at least 0.7 were considered to have high probability of being correct, regardless of other parameters (47). Over 580 different peptides were detected, and proteins were identified with at least two peptides of distinct sequence.

Nuclear staining of 3T3-L1 adipocytes

The 3T3-L1 adipocytes were washed twice with cold PBS, fixed with 3.7% formalin in PBS at room temperature for 10 min, and washed three times with PBS for 15 min each. Specimens were permeabilized with 0.5% Triton X-100 in PBS at room temperature for 5 min and washed as above. To visualize lamin B1, nuclear DNA, and lipid droplets simultaneously, specimens were first blocked with 4% BlockAce (Snowbrand, Tokyo, Japan) in PBS with 0.5% Tween 20 (PBST) at 37°C for 30 min. After brief washing with PBST, specimens were sequentially incubated with primary antibody and AlexaFluor488-conjugated donkey antigoat antibody in 1% BlockAce in PBST at 37°C for 30 min. Nuclear DNA was counterstained with DAPI for 1 min. Finally, lipid droplets were stained with oil red O for 3 min. After rinsing with distilled water, specimens were dried and mounted in antifade reagent (1% 1,4-diazabicyclo [2.2.2] octane, Tris-HCl (pH 8.0), and 90% glycerol). Images were taken by motorized wide-field microscope (Axioplan 2; Zeiss, Oberkochen, Germany) equipped with cooled CCD camera (MicroMAX; Roper). Captured gray images were edited and pseudocolored by ImageJ with plugin (National Institutes of Health, Bethesda, MD). Detection of apoptotic cells was done by using the DeadEnd fluorometric terminal deoxynucleotidyl transferase-mediated deoxyuridine triphosphate nick-end labeling (TUNEL) system (Promega) according to the manufacturer's instructions.

Binding assay of MFG-E8 to phospholipids and apoptotic Jurkat T cells

MFG-E8 binding to solid-phase phospholipid was performed as described previously (25). Briefly, after washing, adiposomes prepared from 3T3-L1 adipocyte-conditioned medium (d 10, on 90-mm dish) were

dissolved in 100 μ l PBS and were added to wells, followed by incubation at 4°C overnight. The plates were then incubated with anti-MFG-E8 antibody and peroxidase-labeled goat antirabbit IgG as the secondary antibody, and peroxidase activity was measured.

Jurkat T cells were cultured in RPMI 1640 supplemented with 10% FCS. Apoptosis was induced with 0.5 μ g/ml staurosporine (Sigma) for 3 h. Apoptotic and nonapoptotic cells were incubated with the adiposome fractions at 37°C for 1 h. Cells were washed three times with PBS and fixed with 2% paraformaldehyde at room temperature for 20 min. After washing with PBST, cells were blocked in PBS containing 2% BSA at room temperature for 30 min. After brief washing with PBST, cells were sequentially reacted with anti-MFG-E8 antibody, AlexaFluor488-conjugated goat antirabbit antibody, and propidium iodide. Finally, cells were washed three times with PBST and twice with distilled water and observed with fluorescence microscopy as above.

Care of mice and tissue preparation

C57BL/6 mice (male, 4 wk old) purchased from Japan SLC (Hamamatsu, Japan) were maintained at 25°C under a 12-h light, 12-h dark cycle (lights on from 0600–1800 h) according to the Mie University guideline for animal study. The mice were fed laboratory chow (rodent diet EQ, Japan SLC) for 1 wk to stabilize their metabolic condition. Then mice were allowed *ad libitum* access to tap water and either of the following synthetic diets for 8 wk: a low-fat (LF) diet containing 5% (wt/wt) corn oil, 25% casein, 40.8% corn starch, 20% sucrose, 0.3% D,L-methionine, 3.5% minerals, 1% vitamins, 4% cellulose, 0.4% choline chloride or a high-fat (HF) diet containing 5% (wt/wt) corn oil, 30% lard, 25% casein, 10.8% corn starch, 20% sucrose, 0.3% D,L-methionine, 3.5% minerals, 1% vitamins, 4% cellulose, 0.4% choline chloride. Plasma glucose, triglyceride, and cholesterol were determined using commercial kits from Wako Pure Chemicals.

Epididymal adipose tissue was excised under anesthesia, finely chopped, and digested with 10 ml of 1 mg/ml type I collagenase (C-0130; Sigma) in Krebs-Henseleit buffer per 1 g tissue at 37°C for 30 min. After centrifugation at 300 \times g for 5 min, adipocytes were separated from the SV fraction. Both fractions were washed three times and subjected to RNA preparation as below.

Northern blotting and quantitative real-time PCR

Total RNA was isolated from epididymal adipose and other tissues, and fractionated cells using Trizol reagent (Invitrogen). Aliquots (10 μ g) were separated on denatured agarose gels and blotted onto nylon membranes. The membrane was hybridized with the MFG-E8 and 36B4 cDNA probe, which had been labeled with [α -³²P]dCTP using Rediprime II (Amersham) and purified with a ProbeQuant G-50 microcolumn (Amersham), in Ultra-hyb buffer (Ambion Inc., Austin, TX) at 42°C overnight. The membrane was washed and exposed to x-ray films.

Total RNAs prepared from tissues and adipocyte and SV fractions were reverse transcribed using a cDNA synthesis kit (SuperScript III first-strand synthesis system for RT-PCR; Invitrogen) and used for quantitative real-time PCR on a BioFlux LineGene (TOYOBO, Osaka, Japan) using a SYBR Green real-time PCR master mix (TOYOBO) according to the manufacturer's instructions. The housekeeping transcript, elongation factor-1 α (EF-1 α), was used as an internal control. The primers used for each gene are as follows: MFG-E8, 5'-TCTGGTGA CTCTGTGACTC-3' and 5'-AACC GGTTTCACAGTGGATG; adiponectin, 5'-GATGGCAGAGATGGCAGTCC-3' and 5'-CTTGCCAGTGCTGCCGTCAT-3'; CD68, 5'-CTTCCCACAGGCAGCAGCAG-3' and 5'-AATGATGAGAGGCAGCAAGAGG-3'; and EF-1 α , 5'-CTCAGGTGATTATCCTGAACCATC-3' and 5'-AACAGTCTGAGACCGTCTTCCA-3'. The PCR products were evaluated by inspection of their melting curves (data not shown).

Results

Secretion of microvesicles by 3T3-L1 adipocytes

So far, limited numbers of cell types have been reported to secrete microvesicles. To examine whether adipocytes secrete such microvesicles, 3T3-L1 cells were selected as a model of adipocytes. Conditioned medium was harvested and assessed by immunoblotting with anti-MFG-E8 anti-

body, because MFG-E8 has been shown to be present in a relatively high amount in microvesicles secreted by dendritic cells (21, 23–26) and mammary epithelial cells (27). As shown in Fig. 1A, MFG-E8 was clearly detected in the microvesicle fractions secreted by 3T3-L1 adipocytes, whereas NIH3T3 cells did to a lesser extent. In addition, rat primary adipocytes also secreted MFG-E8-containing microvesicles. Focusing on the 3T3-L1 and rat primary adipocytes, more than 85% of secreted MFG-E8 was recovered in the precipitates after ultracentrifugation (Fig. 1B).

Microscopic observation of microvesicles secreted by 3T3-L1 adipocytes

Transmission electron microscopic analysis revealed that microvesicle secretion indeed occurred and that the size of the membrane vesicles was not uniform and both smaller exosome-like vesicles and larger ones of more than 100 nm in diameter were observed (Fig. 2A, panel a). Much larger vesicles of nearly 1 μm in diameter were also present (Fig. 2A, panel b). MFG-E8 was confirmed to be present on the vesicles with exosomal and larger shed membrane features, as revealed by immunoelectron microscopic analysis (Fig. 2B). These results suggest that 3T3-L1 adipocyte-derived microvesicles are generated by membrane shedding as well as by multivesicular body-mediated exosomal secretion. We refer to these microvesicles as adiposomes.

Adiposome-associated protein components in the course of 3T3-L1 differentiation

Conditioned medium was continuously collected every 2 d in the course of the differentiation process of 3T3-L1 cells. Microvesicle/adiposome fractions were prepared by ultracentrifugation as described and assessed by immunoblotting. MFG-E8 was detected in the microvesicle fractions before the cells became differentiated (Fig. 3A). After differentiation in-

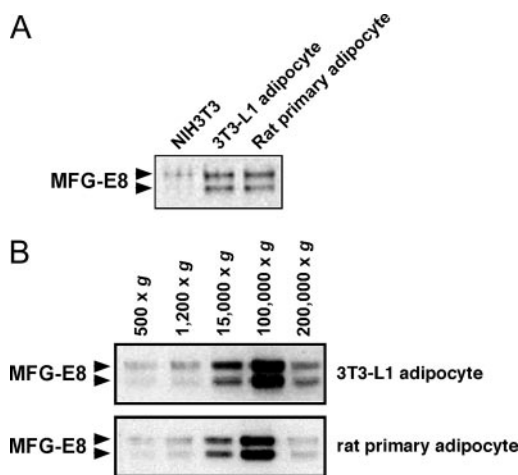


FIG. 1. Secretion of MFG-E8-associated microvesicles by 3T3-L1 adipocytes. A, Microvesicle fractions were prepared from 2-d conditioned media (6 ml per 90-mm dish) of indicated cells as described under *Materials and Methods* and then probed with anti MFG-E8 antibody. B, Conditioned media (6 ml per 90-mm dish) of 3T3-L1 (d 8) and rat primary adipocytes were differentially centrifuged under indicated conditions, and resultant pellets were separated and probed with anti-MFG-E8 antibody.

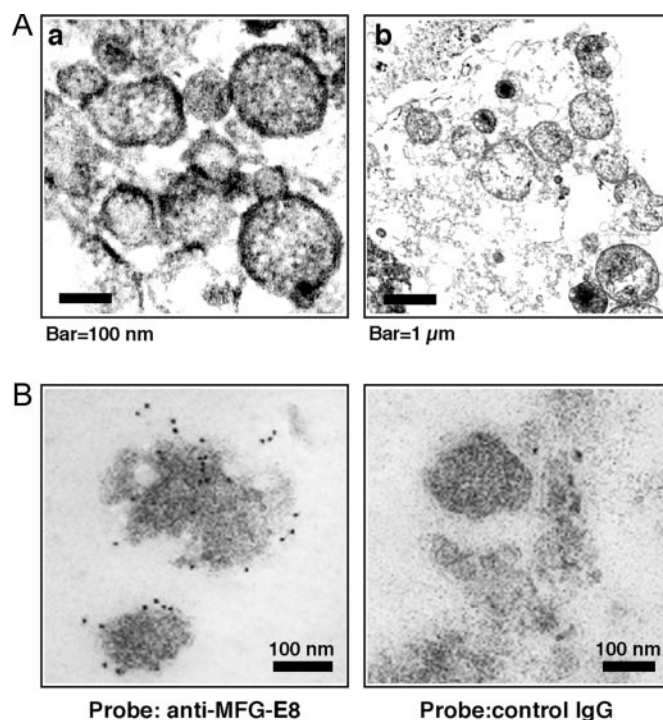


FIG. 2. Ultrastructural analysis of microvesicles secreted by 3T3-L1 adipocytes. A, Purified microvesicles secreted by 3T3-L1 adipocytes were fixed and embedded in EPON812. After a negative staining, ultrathin sections were observed by transmission electron microscopy. B, Purified microvesicles were placed on electron microscopy grids, fixed, contrasted, and embedded. Ultrathin sections were probed with affinity-purified anti-MFG-E8 or control rabbit IgG after incubation with ImmunoGold-labeled secondary antibody.

duction, 3T3-L1 adipocytes continuously secreted MFG-E8-containing adiposomes except for d 2 due to unknown reasons. c-Src is known to be localized in cytosol and attached to the inner leaflet of plasma membrane through myristoylation as well as palmitoylation (49). c-Src was detected in the cell lysates throughout the differentiation process. Surprisingly, this protein was also present in the adiposomes while also slightly detected in the microvesicle fractions before differentiation. Most strikingly, plasma membrane integral proteins caveolin-1 and -2 were found to be in the adiposomes 8 d after differentiation, although substantial amounts of both proteins were expressed in the preadipocytes. A related protein, flotillin-2 behaved in a similar manner. HSP70 and histone H2B were also found to be present in the adiposomes and increased with differentiation, although nearly constant amounts of the proteins were detected in the cell lysates. Protein content in the microvesicle fractions increased as differentiation proceeded and was estimated to be about 10 μg per adipocyte on a 90-mm dish (Fig. 3B).

The 3T3-L1 adipocytes express and secrete substantial amounts of adipocytokines such as adiponectin and resistin. We addressed the presence of these protein factors in the adiposome fractions. As shown in Fig. 3A, adiponectin was found to be present in the adiposome fractions, whereas resistin was hardly detected. Adiponectin exists as at least three homomeric complexes, trimeric, hexameric, and high-molecular-weight forms (50). Interestingly, the level of the

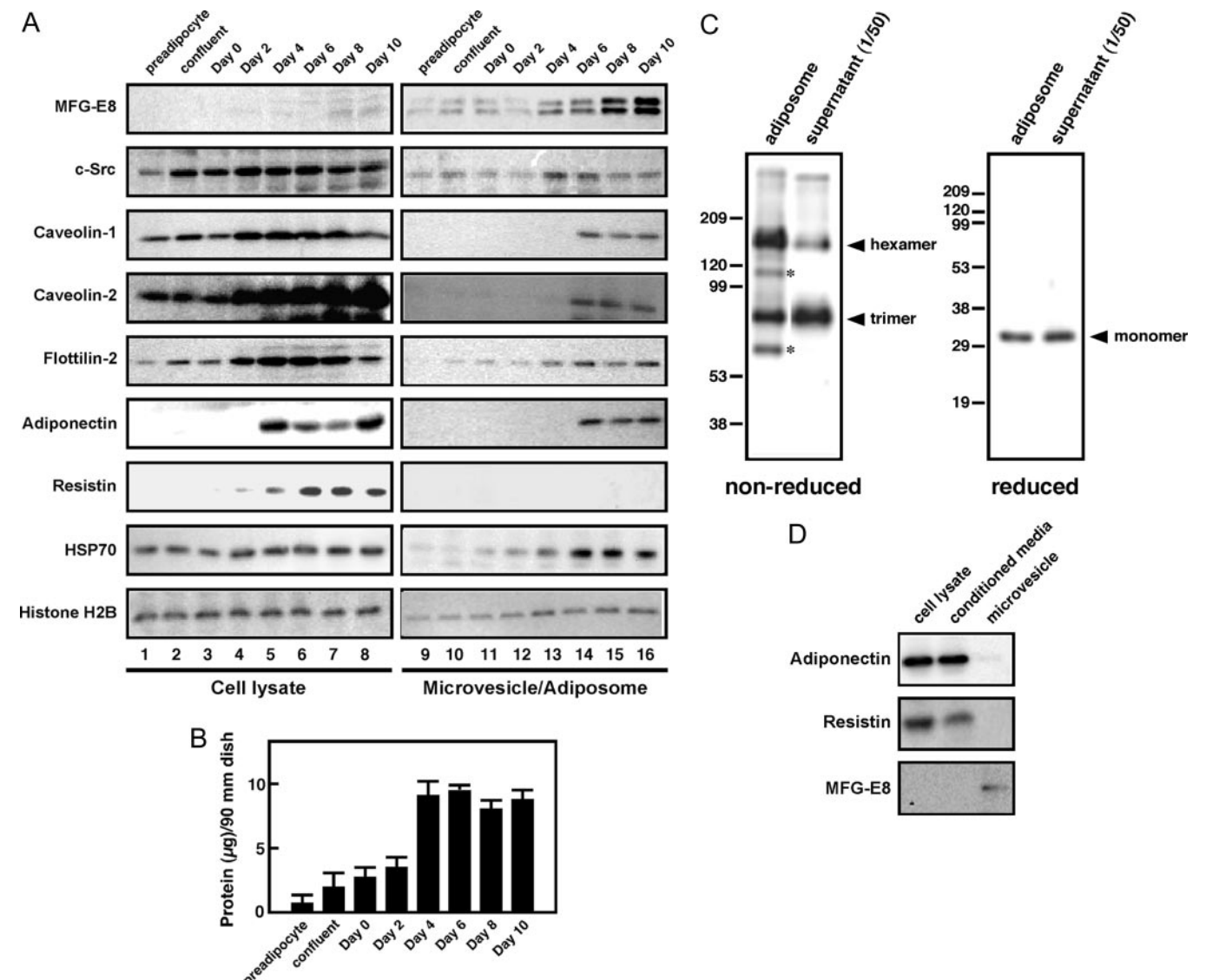


FIG. 3. Time-course analysis of microvesicle/adiposome secretion by 3T3-L1 cells. **A**, Conditioned medium (6 ml per 90-mm dish) were harvested on the indicated days and ultracentrifuged for microvesicle/adiposome preparation, and simultaneously cells were lysed. Microvesicle/adiposome fractions and cell lysates were separated and probed with indicated antibodies. **B**, Microvesicle/adiposome fractions were suspended in PBS and briefly sonicated, and then protein contents were determined by bicinchoninic acid assay. **C**, 3T3-L1 adipocyte (d 10) conditioned medium (6 ml per 90-mm dish) was fractionated into adiposome and supernatant by ultracentrifugation. Whole pellet (adiposome fraction) and an aliquot of the supernatant (1/50) were separated by SDS-PAGE under the nonreduced or reduced condition followed by Western blotting with antiadiponectin antibody. Monomeric, trimeric, and hexameric forms of adiponectin are indicated by arrowheads. Two discrete bands in the adiposome fraction are indicated by asterisks. **D**, Expression plasmids bearing mouse adiponectin and resistin were transfected to HEK293 cells as described under *Materials and Methods*. The 2-d conditioned medium was harvested and subjected to microvesicle preparation. An aliquot of the conditioned media (1/50) and cell lysate (1/20) and a whole microvesicle fraction were probed with the indicated antibodies.

hexameric form was higher than that of the trimeric one in the adiposome fraction upon separation under the reduced condition (Fig. 3C). In addition, two discrete bands also were detected in the adiposome fraction. On the contrary, the trimeric form was dominant in the supernatant. When separated under the reduced condition, only monomeric adiponectin was detected in both fractions.

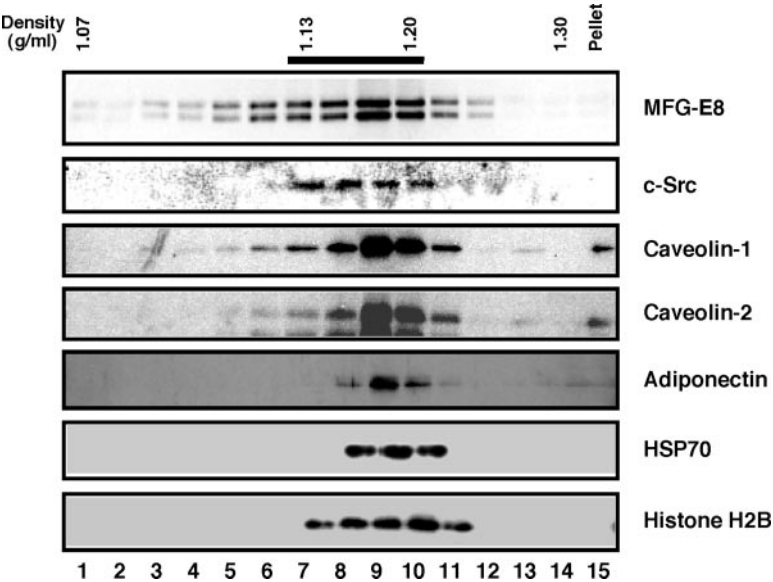
When adiponectin and resistin were transiently overexpressed in HEK293 cells, none of these protein factors was recovered in the microvesicle fractions prepared by ultracentrifugation, although the proteins were indeed expressed and detected both in the cell lysates and conditioned medium

(Fig. 3D), suggesting that adiponectin was selectively associated with adiposomes secreted by 3T3-L1 adipocytes.

Subfractionation of adiposomes on sucrose density gradient by ultracentrifugation

To further confirm the presence of the protein components in adiposomes, conditioned medium from d-8 3T3-L1 adipocytes was harvested, and the precipitates after ultracentrifugation were resuspended in PBS and subfractionated on the sucrose density gradient by ultracentrifugation. Each gradient fraction was concentrated by TCA precipitation and

FIG. 4. Separation of adiposomes by sucrose density gradient ultracentrifugation. Adiposome fractions were prepared from conditioned medium (120 ml) of 3T3-L1 adipocytes and suspended in PBS. The suspension was layered on the top of continuous sucrose gradient (10–70% sucrose in PBS) and centrifuged at 200,000 × *g* for 18 h. Fractions were collected from the top of the tube and subjected to TCA precipitation as described under *Materials and Methods*. Each pellet was analyzed by immunoblotting with indicated antibodies. Densities of some fractions were indicated on the top of the panel. Fractions corresponding to exosomes are indicated by a horizontal bar.



assessed by immunoblotting with the indicated antibodies. MFG-E8 was detected in the fractions with broad densities peaked around 1.13–1.22 g/ml (Fig. 4), which has been reported for exosomes (51). Such distribution was also true for other proteins including adiponectin.

Proteomic analysis of adiposome protein components by HPLC/mass spectrometry

To further characterize the protein components of the purified adiposomes, the sucrose density fractions corresponding to fractions 8–10 of Fig. 4 were recovered, combined, separated by SDS-PAGE, and visualized by silver staining. The same sucrose density fractions derived from conditioned media of 3T3-L1 preadipocytes were also prepared as control. As shown in Fig. 5, distinct sets of adiposomal protein components derived from adipocytes (d 10) were detected. These adiposome fractions were directly trypsinized and fractionated by HPLC followed by analysis with mass spectrometry. Overall, 98 different proteins were identified (Table 1). In addition to MFG-E8, exosomal proteins such as tetraspanins (CD9 and CD63), heat shock proteins (Hsp70 and Hsp84), cytoskeletal proteins (actin and tubulin), enzymes (enolase and pyruvate kinase), and cytosolic proteins (annexin II and galectin-3) were identified (52). Of note, extracellular matrix and its related proteins such as collagens and fibronectin, nuclear proteins such as histones, and ribosomal proteins were frequently identified.

Distribution of adiposome-associated proteins in the 3T3-L1 conditioned medium

MFG-E8 possesses a signal sequence (53) and is therefore believed to be secreted through the endoplasmic reticulum/Golgi pathway. To address the distribution of MFG-E8 secreted by 3T3-L1 adipocytes, cells were incubated in DMEM containing 0.5% FCS for 24 h. Conditioned medium was harvested and subjected to adiposome preparation by ultracentrifugation. Resultant supernatant was retained, and the protein contents were recovered by TCA precipitation. Expression of each protein component in cell lysates was also

determined by immunoblotting followed by densitometric analysis. As shown in Fig. 6, MFG-E8 as well as c-Src, caveolin-1 and -2, HSP70, and histone H2B were detected only in the adiposome fraction of conditioned medium. By contrast, adiponectin (5%) was distributed in the adiposome fraction and most of the remainder recovered in the supernatant (95%). Microvesicles were judged to be produced by viable cells, because intact nuclei were observed by DAPI and lamin B1, an intranuclear protein, staining (Fig. 6C). In addition, TUNEL-positive cells were scarcely detected (Fig. 6D). Resistin was detected only in the supernatant, consistent with the above data (Fig. 3). The majority of the proteins except for MFG-E8 were detected in cell lysates, suggesting that mem-

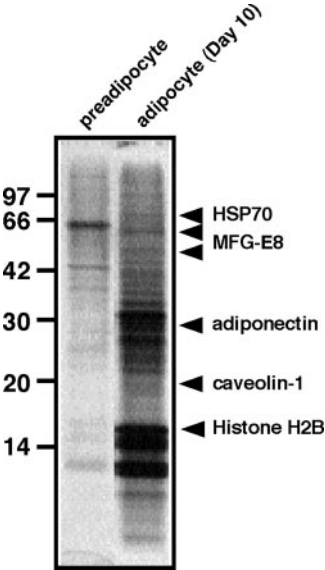


FIG. 5. Protein components of microvesicles/adiposomes. Microvesicles/adiposomes derived from 3T3-L1 preadipocytes and adipocytes (d 10) were purified on sucrose density gradients as described in Fig. 4. The gradient fractions 8–10 were combined and separated by SDS-PAGE followed by visualization with silver staining. Several proteins are indicated based on the immunoblotting data.

TABLE 1. Adiposome protein components derived from 3T3-L1 adipocytes

Identification	Accession no.	Expect	Molecular weight
Extracellular matrix-related proteins			
Collagen, type I, α 1	CAI23970	4.34E-11	137,948.2
Collagen, type I, α 2	BAE36029	3.49E-10	116,797.2
Collagen, type VI, α 1	AAH02194	6.29E-13	44,464.8
Collagen, type VI, α 2	Q02788	1.45E-08	109,743.4
Collagen, type VI, α 3	AAD01978	6.87E-12	185,668.1
Tenascin C	CAD83049	2.83E-10	91,148.3
Fibronectin	P11276	5.22E-14	272,316.2
Laminin α 4	AAC52982	7.54E-11	201,459.8
Nidogen	CAA32642	2.49E-08	136,438.5
Nidogen-2	BAE37706	3.82E-06	153,845.8
Elastin microfibril interfacier 1	BAE33288	2.00E-09	107,517.5
Procollagen-lysine, 2-oxoglutarate 5-dioxygenase 1	BAE34174	1.10E-08	45,102.5
Procollagen C-proteinase enhancer protein	BAE35077	4.83E-11	50,137.1
Integral membrane protein TAPA-1	AAB19417	1.12E-09	25,811.2
Perlecan	XP_919288	1.19E-09	279,675.4
Carbohydrate/lipid metabolism or transport			
Fatty acid synthase	BAE42492	1.86E-09	236,733.6
Long-chain acyl-CoA synthetase	P41216	4.85E-08	77,873.5
Lipoprotein lipase	BAE31986	1.68E-09	53,115.8
Enolase 1	AAH04017	8.36E-10	38,275.5
Enolase 3	CAJ18401	8.36E-10	46,968.3
Pyruvate carboxylase	BAE41902	5.90E-11	129,748.8
Pyruvate kinase M	BAA07457	2.18E-10	57,824.2
ATP synthase β -subunit	AAB86421	1.66E-10	56,344.6
NADP-dependent oxidoreductases	BAC37895	4.22E-11	106,429.9
Phosphoglycerate kinase 1	P09411	4.93E-09	44,508.0
NADP-dependent malic enzyme	XP_923436	3.44E-06	61,499.9
Citrate synthase	AAH13554	6.05E-07	51,703.4
Malate dehydrogenase	CAA30274	1.30E-07	35,573.8
Aldehyde dehydrogenase family 6, subfamily A1	BAE41702	1.58E-07	57,916.6
Glycosyl hydrolases family 31	BAC65483	4.99E-05	87,740.3
Isocitrate/isopropylmalate dehydrogenase	AAH34273	7.88E-06	31,441.8
Fatty acid binding protein 3	BAE24952	6.10E-04	14,809.7
Fatty acid binding protein 4	CAJ18597	1.37E-06	14,640.5
Secreted and transmembrane proteins			
MFG-E8	BAE42274	6.80E-09	51,235.8
Adiponectin	BAC30866	3.60E-08	26,734.2
Fasting-induced adipose factor	AAF86342	2.15E-05	45,510.8
CD9	AAH70474	2.43E-08	25,240.9
CD63	XP_919469	1.19E-06	25,721.3
Integral membrane protein TAPA-1	AAB19417	1.12E-09	25,811.2
Clathrin heavy chain	BAE25402	1.65E-10	114,171.1
MMP-2	AAH70430	4.22E-07	74,054.9
MMP-9	XP_925466	1.47E-08	98,495.4
Coagulation factor II	AAH13662	2.94E-09	70,223.8
Coagulation factor V	BAE23393	8.52E-08	115,696.3
Fibulin 2	AAD34456	1.18E-13	131,874.2
Fibulin 4	NP_067449	3.40E-07	49,419.3
Annexin II	XP_622573	3.86E-10	32,578.7
Complement C3	P01027	4.68E-11	186,364.1
Heat shock/chaperone proteins			
Hsp1 (chaperone)	AAI06113	4.14E-06	59,388.1
Hsp60	XP_925296	2.36E-08	21,213.2
Hsp70	XP_930845	2.40E-09	70,926.4
Spermatid-specific Hsp70	BAA32524	1.86E-09	12,129.2
Hsp75	BAE39316	7.89E-08	80,144.6
Hsp84	P11499	2.31E-08	83,273.2
TCP-1 chaperone family, β subunit	BAA95054	4.29E-12	52,435.8
TCP-1 chaperone family, γ subunit	BAE42283	2.39E-08	31,461.3
TCP-1 chaperone family, ϵ subunit	BAC97866	9.84E-09	59,687.1
Ubiquitin/proteasome-related			
26S Proteasome α 1	BAE40184	1.27E-08	20,176.6
26S Proteasome β 3	XP_920004	1.15E-05	18,764.5
26S Proteasome β 5	O55234	1.25E-11	22,952.4
26S Proteasome Rpn13	BAE42495	3.12E-09	38,171.5
Ubiquitin-activating enzyme E1	BAE25369	5.98E-09	117,734.1
Nuclear proteins			
Histone H1t	NP_034507	9.31E-07	21,626.2

TABLE 1. Continued

Identification	Accession no.	Expect	Molecular weight
Histone H1.3	BAE33250	8.29E-06	22,068.2
Histone H1.5	BAB32001	2.58E-06	22,282.2
Histone H2A	AAH10564	3.13E-09	14,993.3
Histone H2B	XP_214483	8.29E-07	16,561.9
Histone H4	XP_911558	3.82E-07	18,585.9
40S ribosomal protein SA	XP_909595	1.33E-09	8,979.7
40S ribosomal protein S8	XP_890310	1.28E-07	37,564.0
60S ribosomal protein L7	CAA41028	4.49E-07	17,723.7
60S ribosomal protein L18a	BAE40206	5.23E-07	20,619.8
Cytoskeleton			
Actr1b protein	AAH24861	2.33E-09	19,597.2
β-Actin	BAB40317	2.37E-10	14,973.5
Tubulin α2	XP_898880	4.20E-08	28,075.8
Tubulin β2	XP_917827	3.58E-08	49,783.9
Tubulin β5	BAE30573	2.67E-05	42,127.3
Membrane transport and fusion			
Annexin II	XP_622573	3.86E-10	32,578.7
Annexin V	BAE31952	7.46E-07	35,716.2
Miscellaneous			
Galectin 1	AAH02063	3.78E-10	14,868.2
Galectin 3	BAE31013	6.02E-10	64,463.8
EF-1α	XP_921527	1.97E-08	19,617.0
EF-2	BAC28120	1.54E-06	95,195.9
Translation initiation factor 4A, isoform 1/2	XP_929093	9.20E-04	37,370.3
Major vault protein	AAL02325	3.35E-09	95,865.3
14-3-3β	AAC14343	1.26E-12	28,078.9
Valosin containing protein	BAC27119	3.87E-09	89,313.8
Dynein heavy chain	NP_084514	2.44E-08	531,689.6
Albumin	BAC34145	2.95E-08	6,867.8
Sex-limited protein (Slp)	S54784	4.36E-08	192,699.1
α ₂ -Macroglobulin	AAH72642	1.47E-08	164,221.6
H-2 class I histocompatibility antigen α-chain	P03991	2.71E-07	41,077.7
Benzodiazepine receptor	AAH02055	5.83E-07	18,772.6
Proline arginine-rich end leucine-rich repeat	AAH19775	8.81E-07	43,265.1
Thbs2	AAO16244	1.05E-06	129,798.0
Glyceraldehyde-3-phosphate dehydrogenase (GAPDH)	XP_894041	3.62E-13	54,928.0
Semicarbazide-sensitive amine oxidase	AAD09199	6.46E-06	84,481.4
Activated protein kinase C receptor	AAG29506	2.19E-07	32,989.3
Glutathione S-transferase, π2	BAC37560	5.37E-08	22,629.6
Lysyl oxidase-2	AAB86802	3.75E-07	12,252.8

Adiposomal fractions as shown in Fig. 5 were trypsinized, fractionated by HPLC, and analyzed by mass spectrometry for peptide mass fingerprints.

brane-associated, integral, and nuclear proteins were not secreted due to cell death and lysis.

Binding of MFG-E8 in the adiposomes to phospholipids and apoptotic cells

MFG-E8 has been reported to bind to PS and apoptotic cells (27, 28, 30). To address that MFG-E8-associated adiposomes might have such activity, an ELISA-based phospholipid binding assay was done. As shown in Fig. 7A, MFG-E8 in the adiposomes exhibited significant binding activity to PS but not phosphatidylcholine. Such binding activity was not detected when the supernatant fraction was applied. MFG-E8 in the adiposomes also was shown to bind to apoptotic but not nonapoptotic Jurkat T cells (Fig. 7B).

Redox-dependent induction of MFG-E8-associated adiposomes

To elucidate physiological roles of adiposome, 3T3-L1 adipocytes were cultured in the medium containing high (4500 mg/liter) or low (1000 mg/liter) glucose. When cultured in

the high-glucose medium, considerable amounts of MFG-E8 and caveolin-1 were detected in the adiposomes (Fig. 8, A and B). A decrease in medium glucose concentration (1000 mg/liter) significantly diminished MFG-E8 in the adiposomes, whereas caveolin-1 was unchanged. Secretion of resistin but not adiponectin was dramatically reduced when cultured in the low-glucose medium (Fig. 8C), as previously reported (54).

It has recently been reported that hyperglycemia potentiates H₂O₂ production in adipocytes (55), suggesting redox-dependent regulation of MFG-E8-associated adiposomes. When 3T3-L1 adipocytes were cultured in the high-glucose medium with antioxidant NAC, MFG-E8 in the adiposomes significantly decreased in a dose-dependent manner (Fig. 8D). Antioxidant activity of NAC was confirmed by measuring ROS production in the cells (Fig. 8E). ROS production upon culture in the low-glucose medium was comparable to that in the high-glucose medium supplemented with 10 mM NAC. Thus, MFG-E8-associated adiposomes reflected the ROS generated in the cells.

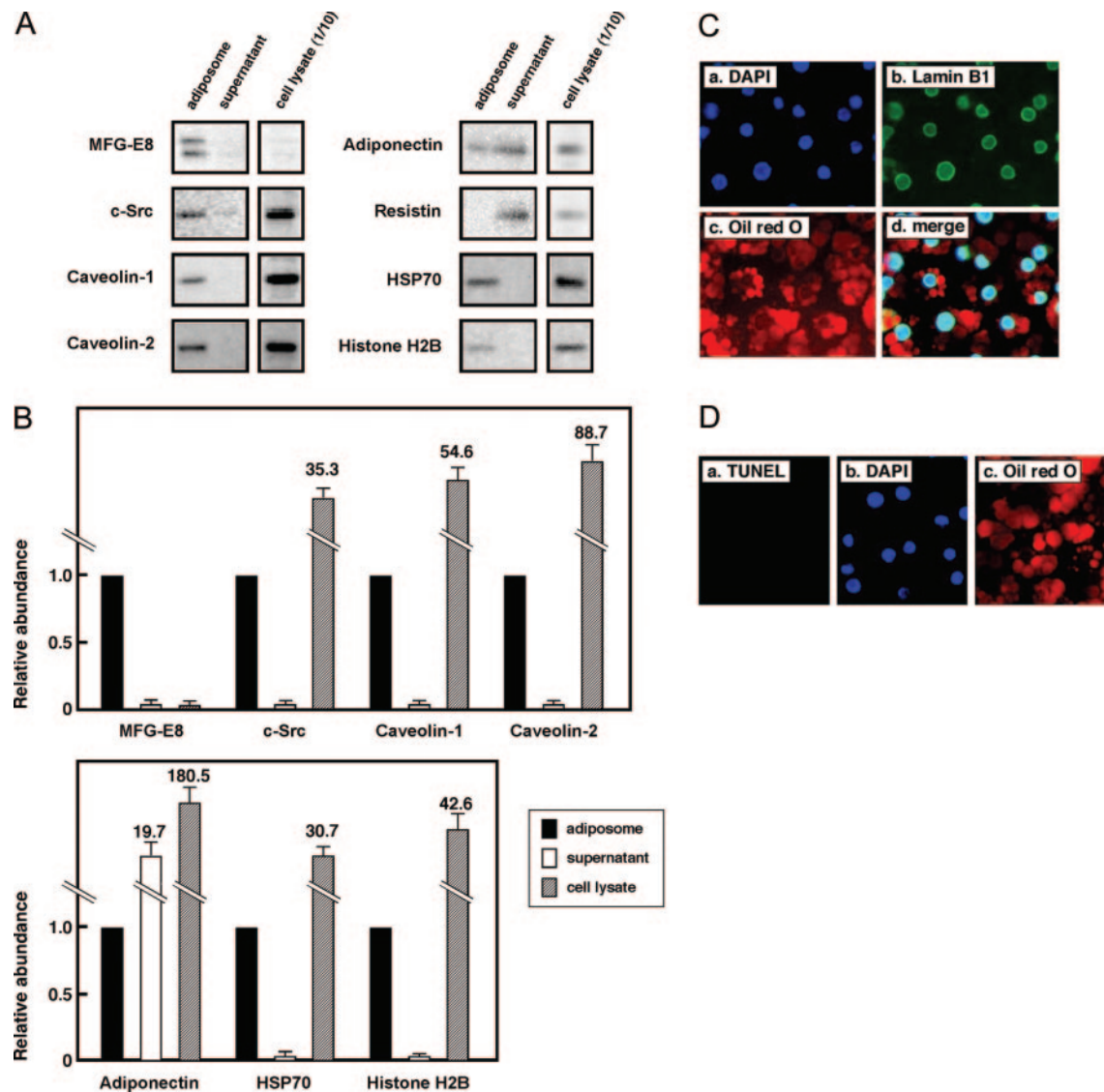


FIG. 6. Distribution of adiposome-associated proteins in the 3T3-L1 adipocyte-conditioned medium. **A**, 3T3-L1 adipocytes were conditioned in DMEM containing 0.5% FCS for 24 h. Conditioned medium was harvested and ultracentrifuged for adiposome preparation. Resultant supernatant was subjected to TCA precipitation to recover nonadiposomal proteins. After harvest of conditioned medium, cells were lysed. Whole adiposome and supernatant fractions and an aliquot of cell lysates (1/10) were immunoblotted with indicated antibodies. **B**, The data in **A** were densitometrically quantitated, where the value for cell lysate was multiplied by 10 and the value for adiposome fraction was set as 1. Results are expressed as means + SEM for three independent experiments, and mean values are indicated. **C**, 3T3-L1 adipocytes were fixed, probed with antilamin B1 antibody, and counterstained with DAPI and oil red O. Bound antilamin B1 antibody was visualized with AlexaFluor488-conjugated donkey antigoat antibody. **D**, Detection of apoptotic cells was done by using the DeadEnd fluorometric TUNEL kit. Cells were counterstained with DAPI and oil red O.

Hormonal induction of MFG-E8-associated adiposomes

In obese animals and human subjects, plasma insulin and TNF- α levels are elevated. Next we addressed the effect of these hormones on the adiposome secretion by 3T3-L1 cells. Insulin treatment of 3T3-L1 cells in the high-glucose medium increased MFG-E8 in the adiposomes (Fig. 9A). TNF- α also up-regulated MFG-E8 in a dose-dependent manner (Fig. 9B). In both cases, the abundance of caveolin-1 was also increased.

Up-regulation of MFG-E8 in the adipose tissue of diet-induced obese mice

To address the physiological relevance of adiposomes *in vivo*, expression of MFG-E8 in the adipose tissue of diet-

induced obese mice was examined, where oxidative stress is induced (46). C57BL/6 mice were fed HF or LF diet for 9 wk. Several parameters are summarized in Table 2. Final body weight, body weight gain, and epididymal fat weight of the HF diet group were significantly higher than those of the LF group. Plasma glucose and cholesterol level of the HF group also were significantly higher than those of the LF group. Interestingly, MFG-E8 mRNA was strongly up-regulated in the epididymal adipose tissues upon HF diet intake, compared with the LF diet (Fig. 10A). Consistently, more MFG-E8 protein was clearly detected in the adipose tissues of HF-induced obese mice (Fig. 10B). MFG-E8 was shown to be expressed predominantly in adipocyte fraction, whereas

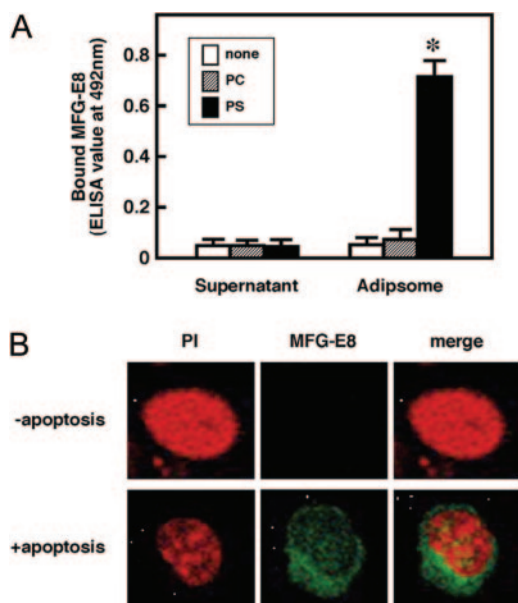


FIG. 7. Binding of MFG-E8-associated adiposomes to PS and apoptotic Jurkat T cells. A, Adiposomes dissolved in PBS were added to the micro-well plates, which had been coated with PS or L- α -phosphatidylcholine. Bound MFG-E8 was detected as described under *Materials and Methods*. The data are shown as mean \pm SD of four independent experiments. B, Staurosporine-induced apoptotic and nonapoptotic Jurkat T cells were incubated with adiposomes and processed as described under *Materials and Methods*. Bound MFG-E8 antibody was visualized with AlexaFluor488-conjugated goat antirabbit antibody, and nucleus was counterstained with propidium iodide.

CD68 and adiponectin were primarily expressed in SV and adipocyte fractions, respectively (Fig. 10C). Moreover, expression of MFG-E8 was highly specific in the epididymal adipose tissue of HF-induced obese mice and was by more than 50 times higher than that in liver (Fig. 10D), although MFG-E8 was originally identified as one of the major components of milk fat globule membrane proteins.

Discussion

The importance of microvesicle secretion and the release of protein components from the cell via this mechanism has now been described in a variety of species and physiological conditions and is thought to be crucial in development, generating signaling gradients in *Drosophila* (56, 57), vertebrate bone growth (58, 59), platelet activation (60), and in the immune system (14, 61, 62). The specific importance of vesicle shedding in tumor cells has also been addressed (20, 63–66). It has been shown to occur in tumor cells *in vitro* and *in vivo* and is associated with malignancy. It is likely that vesicle shedding and, more importantly, the factors released by vesicle shedding, are vital to tumor survival and growth, because it is by the release of such factors that tumors condition their microenvironment, regulate metastasis, and evade immune surveillance.

Based on the presence of an exosomal marker protein, MFG-E8, we found that 3T3-L1 adipocytes release microvesicles, named adiposomes. Identification of microvesicles as exosomes and plasma membrane-derived vesicles relies on various criteria such as their size and density and the existence of

component proteins. Adiposomes secreted by 3T3-L1 adipocytes exhibited heterogeneity in size and comprised both smaller exosome-like and larger membrane vesicles by electron microscopy (Fig. 2). In addition to MFG-E8, many other exosomal proteins were also revealed in the adiposomes by immunoblotting (Figs. 3, 4, and 6) as well as proteomic analysis (Table 1). These results support the idea that adipocytes secrete both types of micromembranes. It has been reported that platelets and tumor cells also secreted vesicles with exosomal features in addition to plasma membrane-derived vesicles (60).

Association of a typical adipocytokine, adiponectin, but not resistin, was unexpected (Fig. 3A). Lesser but significant

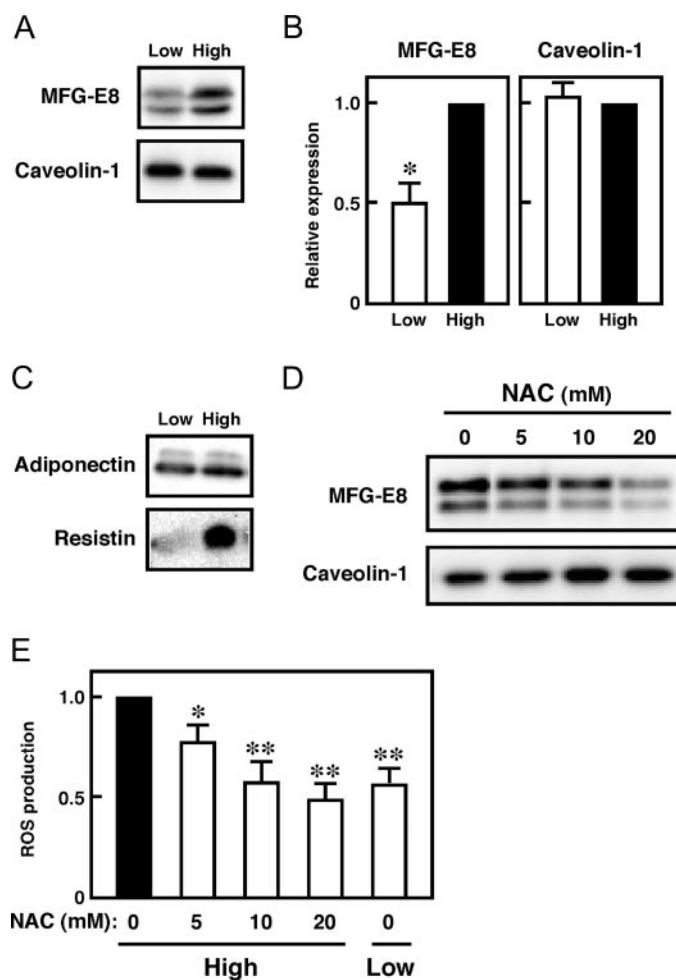


FIG. 8. Redox-dependent regulation of adiposome secretion. A, 3T3-L1 adipocytes were cultured in DMEM containing 1000 mg/liter (low) or 4500 mg/ml (high) glucose supplemented with 10% FCS for 24 h. Adiposomes were separated by SDS-PAGE followed by immunoblotting with indicated antibodies. B, Band intensity of A was densitometrically normalized by ATTO CS analyzer (ATTO, Japan). The intensity level of each band derived from high glucose was set at 1. Results are expressed as means \pm SEM ($n = 3$). *, $P < 0.05$. C, Aliquots of conditioned medium as in A were immunoblotted with indicated antibodies. D, 3T3-L1 adipocytes were cultured in DMEM (4500 mg/ml glucose) supplemented with indicated amounts of NAC for 24 h. Adiposomes were assessed as above. E, ROS production in 3T3-L1 adipocytes cultured under the above conditions was determined as described under *Materials and Methods*. Results are expressed as means \pm SEM ($n = 3$). *, $P < 0.05$; **, $P < 0.01$.

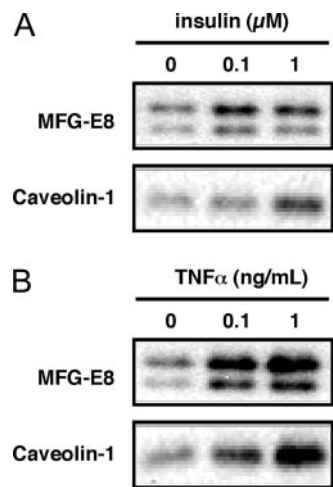


FIG. 9. Hormonal regulation of adiposome secretion. 3T3-L1 adipocytes were cultured in DMEM containing 4500 mg/ml (high) glucose supplemented with 10% FCS in the presence of insulin (A) or TNF- α (B) for 24 h. Adiposomes were separated by SDS-PAGE followed by immunoblotting with indicated antibodies.

amounts of adiponectin were detected in the adiposome fractions compared with the residual supernatant fraction (Fig. 5). In addition to sedimentation by ultracentrifugation, these protein factors were substantially detected in the fractions with density ranges reported for exosomal vesicles (Fig. 4), strongly suggesting that adiponectin actually associated with adiposomes. Adiponectin has a conventional signal sequence at its N-terminal end and is, therefore, thought to be secreted through the endoplasmic reticulum/Golgi pathway. When expressed in nonadipose HEK293 cells, adiponectin could not be recovered in the microvesicle fractions where MFG-E8 was demonstrated to be present, even though high amounts of protein were secreted into cell culture media (Fig. 3D). It has been reported that adiponectin can bind to collagen I, III, and V in a solid-phase binding assay (67). Proteomic analysis frequently hit the presence of collagens in the adiposomes (Table 1), which might suggest anchoring of adiponectin to the adiposomes through collagens. Supporting this speculation, no collagens have been identified in the membrane vesicles secreted by HEK293 cells (data not shown).

MFG-E8 in the adiposomes exhibited binding activity toward PS and apoptotic Jurkat T cells (Fig. 7), as reported for the protein secreted by activated macrophages (28) and mammary epithelial cells (27, 30). These results suggest that MFG-E8-associated adiposomes are also involved in labeling of apoptotic cells for subsequent elimination, although ap-

TABLE 2. Parameters of C57BL/6 mice

	LF diet	HF diet
Initial body weight (g)	20.6 \pm 1.36	21.2 \pm 1.35
Final body weight (g)	38.6 \pm 2.26	44.6 \pm 1.69 ^a
Body weight gain (g)	18.13 \pm 1.47	23.97 \pm 1.35 ^a
Epididymal fat (g)	1.846 \pm 0.239	2.636 \pm 0.237 ^a
Plasma glucose (mg/dl)	214.6 \pm 15.2	270.5 \pm 12.3 ^a
Plasma triglyceride (mg/dl)	95.5 \pm 12.2	116.8 \pm 14.8
Plasma cholesterol (mg/dl)	133.9 \pm 3.3	214.6 \pm 12.0 ^a

Values are expressed as means \pm SEM of six mice.
^a $P < 0.05$ vs. LF.

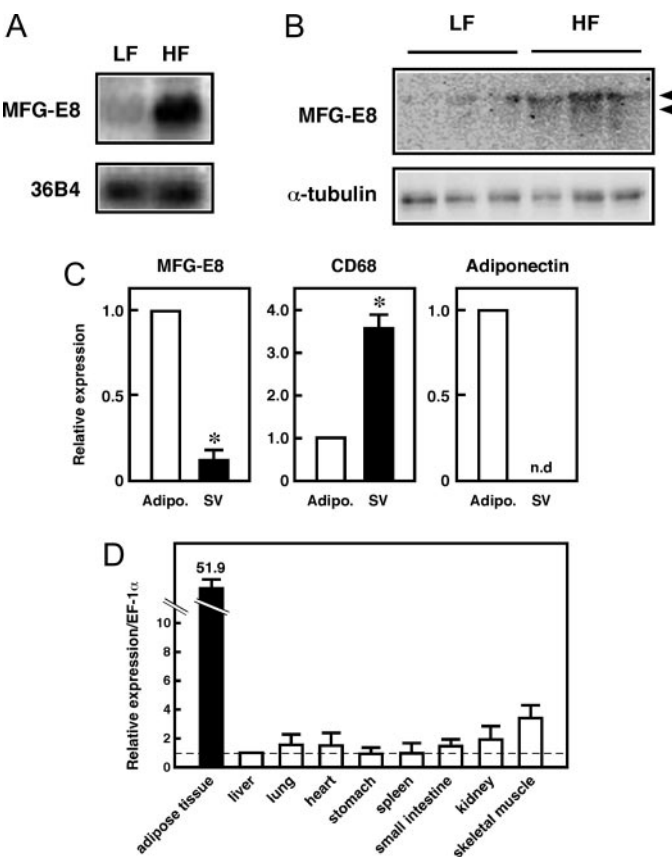


FIG. 10. Up-regulation of MFG-E8 in the adipose tissues of HF-diet-induced obese mice. A, Epididymal adipose tissues of C57BL/6 mice fed on a HF or LF diet were excised, and RNA samples were prepared and processed for Northern blotting as described under *Materials and Methods*. B, Proteins were extracted from adipose tissues of both diet groups (three mice for each diet group), and aliquots (20 μ g) were sequentially immunoblotted with anti-MFG-E8 and anti- α -tubulin antibodies. C, Epididymal adipose tissues of HF-diet-induced obese mice were fractionated into adipocyte (Adipo.) and SV fractions as described under *Materials and Methods*. Relative expressions of MFG-E8, CD68, and adiponectin to EF1- α in both fractions are shown. Results are expressed as means \pm SEM (n = 5). *, $P < 0.01$. D, Relative expression of MFG-E8 to EF1- α in epididymal adipose and other tissues of HF-diet-induced obese mice was estimated by quantitative real-time PCR. The value for liver was set as 1. Results are expressed as means \pm SEM (n = 3), and mean value for epididymal adipose tissue is indicated.

optosis of adipocytes *in vivo* under certain physiological conditions remains unclear.

Adipose function can be easily affected by various physiological conditions, and it has indeed been reported that expression of one of the adipocytokines, resistin, was up-regulated by a high glucose concentration in the cell culture medium (54). In this study, adiposome secretion also was shown to be regulated by glucose. A high glucose concentration induced increased MFG-E8 in the adiposomes (Fig. 8). ROS production was also increased when cultured in the high-glucose medium, and NAC treatment obviously decreased MFG-E8 in the adiposomes. Expression of MFG-E8 was highly up-regulated in epididymal adipose tissues of diet-induced obese C57BL/6 mice (Fig. 10) as well as genetically obese ob/ob and db/db mice (Aoki, N., and Y. Nakagawa, unpublished

observation). It has also been reported that ROS production increases in adipose tissues of HF-diet-induced obese mice (46). Reduced nicotinamide adenine dinucleotide phosphate oxidase components involved in ROS production were also up-regulated in the HF-diet-induced hypertrophic adipose tissue (data not shown). Thus, it is clearly indicated that at least MFG-E8-associated adiposomes are under the redox-dependent control. In addition to redox-dependent control, MFG-E8 was also regulated by humoral factors such as insulin and TNF- α (Fig. 9), both of which are known to be elevated in obese animals and subjects.

Proteomic analysis revealed that MMPs (MMP-2 and MMP-9) were present in the adiposomes (Table 1) and confirmed by zymographic analysis (Aoki, N., R. Yokoyama, and N. Asai, unpublished observation). MMPs have been reported to be involved in adipose tissue enlargement and remodeling as well as adipogenesis (68) and have been shown to be secreted by endothelial cells through membrane shedding (65). It has also been reported that MFG-E8 is involved in angiogenesis as a cofactor of vascular endothelial growth factor (31) and that angiogenesis is tightly associated with adipogenesis (48). Preliminary data showed that MFG-E8 in part colocalized with MMPs in the adiposomes (Aoki, N., R. Yokoyama, and N. Asai, unpublished observation), suggesting that both proteins cooperatively and effectively function in association with adiposomes in adipose hypertrophy. Secreted MFG-E8 was distributed only in the adiposomes (Fig. 6) and was predominantly expressed in the adipocyte fraction (Fig. 10). Moreover, expression of MFG-E8 in the adipose tissue of obese mice was much higher than that in other tissues (Fig. 10). Thus, MFG-E8-associated adiposomes might play an important and possibly specific role in the adipose tissue.

Taken all together, identification of adipocyte-derived microvesicles, adiposomes, is novel to our knowledge. The adiposome might be a potentially useful target in treatment of adipose dysfunctions such as obesity-associated metabolic syndrome.

Acknowledgments

We acknowledge the assistance of Drs. Tatsuro Saito and Katsuzumi Okumura (Graduate School of Bioresources, Mie University) for immunofluorescence microscopic analyses. We thank Drs. Shinji Kihara and Tatsuya Moriyama for providing us with antiadiponectin and antiregulin antibodies, respectively.

Received November 6, 2006. Accepted April 25, 2007.

Address all correspondence and requests for reprints to: Naohito Aoki, Department of Life Sciences, Graduate School of Bioresources, Mie University, 1577 Kurimamachiya-cho, Tsu 514-8507, Japan. E-mail: n-aoki@bio.mie-u.ac.jp.

This work was supported by a Grants-in-Aid for Scientific Research from the Ministry of Education, Culture, Sports, Science and Technology of Japan (to N.A. and T.M.) and the COE program of Graduate School of Bioresources, Mie University.

Disclosure Statement: The authors have nothing to disclose.

References

- Dainiak N 1991 Surface membrane-associated regulation of cell assembly, differentiation, and growth. *Blood* 78:264–276
- Dolo V, Ginestra A, Ghersi G, Nagase H, Vittorelli ML 1994 Human breast carcinoma cells cultured in the presence of serum shed membrane vesicles rich in gelatinolytic activities. *J Submicrosc Cytol Pathol* 26:173–180

- Dainiak N, Sorba S 1991 Intracellular regulation of the production and release of human erythroid-directed lymphokines. *J Clin Invest* 87:213–220
- Dolo V, Pizzurro P, Ginestra A, Vittorelli ML 1995 Inhibitory effects of vesicles shed by human breast carcinoma cells on lymphocyte ^3H -thymidine incorporation, are neutralised by anti TGF- β antibodies. *J Submicrosc Cytol Pathol* 27:535–541
- Dolo V, Ginestra A, Cassara D, Violini S, Lucania G, Torrisi MR, Nagase H, Canevari S, Pavan A, Vittorelli ML 1998 Selective localization of matrix metalloproteinase 9, β_1 integrins, and human lymphocyte antigen class I molecules on membrane vesicles shed by 8701-BC breast carcinoma cells. *Cancer Res* 58:4468–4474
- Poste G, Nicolson GL 1980 Arrest and metastasis of blood-borne tumor cells are modified by fusion of plasma membrane vesicles from highly metastatic cells. *Proc Natl Acad Sci USA* 77:399–403
- Zucker S, Wieman JM, Lysik RM, Wilkie DP, Ramamurthy N, Lane B 1987 Metastatic mouse melanoma cells release collagen-gelatin degrading metalloproteinases as components of shed membrane vesicles. *Biochim Biophys Acta* 924:225–237
- Ginestra A, Monea S, Seghezzi G, Dolo V, Nagase H, Mignatti P, Vittorelli ML 1997 Urokinase plasminogen activator and gelatinases are associated with membrane vesicles shed by human HT1080 fibrosarcoma cells. *J Biol Chem* 272:17216–17222
- Ginestra A, La Placa MD, Saladino F, Cassara D, Nagase H, Vittorelli ML 1998 The amount and proteolytic content of vesicles shed by human cancer cell lines correlates with their in vitro invasiveness. *Anticancer Res* 18:3433–3437
- D'Angelo M, Billings PC, Pacifici M, Leboy PS, Kirsch T 2001 Authentic matrix vesicles contain active metalloproteinases (MMP): a role for matrix vesicle-associated MMP-13 in activation of transforming growth factor- β . *J Biol Chem* 276:11347–11353
- Trams EG, Lauter CJ, Salem Jr N, Heine U 1981 Exfoliation of membrane ecto-enzymes in the form of micro-vesicles. *Biochim Biophys Acta* 645:63–70
- Heijnen CJ, Kavelaars A 1999 The importance of being receptive. *J Neuroimmunol* 100:197–202
- Cooper DN, Barondes SH 1990 Evidence for export of a muscle lectin from cytosol to extracellular matrix and for a novel secretory mechanism. *J Cell Biol* 110:1681–1691
- MacKenzie A, Wilson HL, Kiss-Toth E, Dower SK, North RA, Surprenant A 2001 Rapid secretion of interleukin-1 β by microvesicle shedding. *Immunity* 15:825–835
- Taverna S, Ghersi G, Ginestra A, Rigogliuso S, Pecorella S, Alaimo G, Saladino F, Dolo V, Dell'Era P, Pavan A, Pizzolanti G, Mignatti P, Presta M, Vittorelli ML 2003 Shedding of membrane vesicles mediates fibroblast growth factor-2 release from cells. *J Biol Chem* 278:51911–51919
- Sidhu SS, Mengistab AT, Tauscher AN, LaVail J, Basbaum C 2004 The microvesicle as a vehicle for EMMPRIN in tumor-stromal interactions. *Oncogene* 23:956–963
- Gruenberg J, Maxfield FR 1995 Membrane transport in the endocytic pathway. *Curr Opin Cell Biol* 7:552–563
- Denzer K, Kleijmeer MJ, Heijnen HF, Stoorvogel W, Geuze HJ 2000 Exosome: from internal vesicle of the multivesicular body to intercellular signaling device. *J Cell Sci* 113(Pt 19):3365–3374
- Raposo G, Nijman HW, Stoorvogel W, Liejendekker R, Harding CV, Melief CJ, Geuze HJ 1996 B lymphocytes secrete antigen-presenting vesicles. *J Exp Med* 183:1161–1172
- Zitvogel L, Regnault A, Lozier A, Wolfers J, Flament C, Tenza D, Ricciardi-Castagnoli P, Raposo G, Amigorena S 1998 Eradication of established murine tumors using a novel cell-free vaccine: dendritic cell-derived exosomes. *Nat Med* 4:594–600
- Thery C, Regnault A, Garin J, Wolfers J, Zitvogel L, Ricciardi-Castagnoli P, Raposo G, Amigorena S 1999 Molecular characterization of dendritic cell-derived exosomes. Selective accumulation of the heat shock protein hsc73. *J Cell Biol* 147:599–610
- Mathew A, Bell A, Johnstone RM 1995 Hsp-70 is closely associated with the transferrin receptor in exosomes from maturing reticulocytes. *Biochem J* 308(Pt 3):823–830
- Thery C, Boussac M, Veron P, Ricciardi-Castagnoli P, Raposo G, Garin J, Amigorena S 2001 Proteomic analysis of dendritic cell-derived exosomes: a secreted subcellular compartment distinct from apoptotic vesicles. *J Immunol* 166:7309–7318
- Morelli AE, Larregina AT, Shufesky WJ, Sullivan ML, Stolz DB, Papworth GD, Zahorchak AF, Logar AJ, Wang Z, Watkins SC, Falo Jr LD, Thomson AW 2004 Endocytosis, intracellular sorting, and processing of exosomes by dendritic cells. *Blood* 104:3257–3266
- Veron P, Segura E, Sugano G, Amigorena S, Thery C 2005 Accumulation of MFG-E8/lactadherin on exosomes from immature dendritic cells. *Blood Cells Mol Dis* 35:81–88
- Segura E, Amigorena S, Thery C 2005 Mature dendritic cells secrete exosomes with strong ability to induce antigen-specific effector immune responses. *Blood Cells Mol Dis* 35:89–93
- Oshima K, Aoki N, Kato T, Kitajima K, Matsuda T 2002 Secretion of a peripheral membrane protein, MFG-E8, as a complex with membrane vesicles. *Eur J Biochem* 269:1209–1218

28. Hanayama R, Tanaka M, Miwa K, Shinohara A, Iwamatsu A, Nagata S 2002 Identification of a factor that links apoptotic cells to phagocytes. *Nature* 417:182–187
29. Hanayama R, Nagata S 2005 Impaired involution of mammary glands in the absence of milk fat globule EGF factor 8. *Proc Natl Acad Sci USA* 102:16886–16891
30. Nakatani H, Aoki N, Nakagawa Y, Jin-No S, Aoyama K, Oshima K, Ohira S, Sato C, Nadano D, Matsuda T 2006 Weaning-induced expression of a milk-fat globule protein, MFG-E8, in mouse mammary glands, as demonstrated by the analyses of its mRNA, protein and phosphatidylserine-binding activity. *Biochem J* 395:21–30
31. Silvestre JS, Thery C, Hamard G, Boddaert J, Aguilar B, Delcayre A, Houbbron C, Tamarat R, Blanc-Brude O, Heeneman S, Clergue M, Duriez M, Merval R, Levy B, Tedgui A, Amigorena S, Mallat Z 2005 Lactadherin promotes VEGF-dependent neovascularization. *Nat Med* 11:499–506
32. Matsuzawa Y 2005 White adipose tissue and cardiovascular disease. *Best Pract Res Clin Endocrinol Metab* 19:637–647
33. Koerner A, Kratzsch J, Kiess W 2005 Adipocytokines: leptin-the classical, resistin-the controversial, adiponectin-the promising, and more to come. *Best Pract Res Clin Endocrinol Metab* 19:525–546
34. Shimomura I, Funahashi T, Takahashi M, Maeda K, Kotani K, Nakamura T, Yamashita S, Miura M, Fukuda Y, Takemura K, Tokunaga K, Matsuzawa Y 1996 Enhanced expression of PAI-1 in visceral fat: possible contributor to vascular disease in obesity. *Nat Med* 2:800–803
35. Hotamisligil GS, Shargill NS, Spiegelman BM 1993 Adipose expression of tumor necrosis factor- α : direct role in obesity-linked insulin resistance. *Science* 259:87–91
36. Uysal KT, Wiesbrock SM, Marino MW, Hotamisligil GS 1997 Protection from obesity-induced insulin resistance in mice lacking TNF- α function. *Nature* 389:610–614
37. Fruebis J, Tsao TS, Javarschi S, Ebbets-Reed D, Erickson MR, Yen FT, Bihain BE, Lodish HF 2001 Proteolytic cleavage product of 30-kDa adipocyte complement-related protein increases fatty acid oxidation in muscle and causes weight loss in mice. *Proc Natl Acad Sci USA* 98:2005–2010
38. Yamauchi T, Kamon J, Waki H, Terauchi Y, Kubota N, Hara K, Mori Y, Ide T, Murakami K, Tsuboyama-Kasaoka N, Ezaki O, Akanuma Y, Gavrilova O, Vinson C, Reitman ML, Kagechika H, Shudo K, Yoda M, Nakano Y, Tobe K, Nagai R, Kimura S, Tomita M, Froguel P, Kadowaki T 2001 The fat-derived hormone adiponectin reverses insulin resistance associated with both lipodystrophy and obesity. *Nat Med* 7:941–946
39. Berg AH, Combs TP, Du X, Brownlee M, Scherer PE 2001 The adipocyte-secreted protein Acrp30 enhances hepatic insulin action. *Nat Med* 7:947–953
40. Maeda N, Shimomura I, Kishida K, Nishizawa H, Matsuda M, Nagaretani H, Furuyama N, Kondo H, Takahashi M, Arita Y, Komuro R, Ouchi N, Kihara S, Tochino Y, Okutomi K, Horie M, Takeda S, Aoyama T, Funahashi T, Matsuzawa Y 2002 Diet-induced insulin resistance in mice lacking adiponectin/ACRP30. *Nat Med* 8:731–737
41. Okamoto Y, Kihara S, Ouchi N, Nishida M, Arita Y, Kumada M, Ohashi K, Sakai N, Shimomura I, Kobayashi H, Terasaka N, Inaba T, Funahashi T, Matsuzawa Y 2002 Adiponectin reduces atherosclerosis in apolipoprotein E-deficient mice. *Circulation* 106:2767–2770
42. Matsuda M, Shimomura I, Sata M, Arita Y, Nishida M, Maeda N, Kumada M, Okamoto Y, Nagaretani H, Nishizawa H, Kishida K, Komuro R, Ouchi N, Kihara S, Nagai R, Funahashi T, Matsuzawa Y 2002 Role of adiponectin in preventing vascular stenosis. The missing link of adipo-vascular axis. *J Biol Chem* 277:37487–37491
43. Yamauchi T, Kamon J, Waki H, Imai Y, Shimozawa N, Hioki K, Uchida S, Ito Y, Takakuwa K, Matsui J, Takata M, Eto K, Terauchi Y, Komeda K, Tsunoda M, Murakami K, Ohnishi Y, Naitoh T, Yamamura K, Ueyama Y, Froguel P, Kimura S, Nagai R, Kadowaki T 2003 Globular adiponectin protected ob/ob mice from diabetes and ApoE-deficient mice from atherosclerosis. *J Biol Chem* 278:2461–2468
44. Aoki N, Ishii T, Ohira S, Yamaguchi Y, Negi M, Adachi T, Nakamura R, Matsuda T 1997 Stage specific expression of milk fat globule membrane glycoproteins in mouse mammary gland: comparison of MFG-E8, butyrophilin, and CD36 with a major milk protein, β -casein. *Biochim Biophys Acta* 1334:182–190
45. Wubbolts R, Leckie RS, Veenhuizen PT, Schwarzmann G, Mobius W, Hoernschmeyer J, Slot JW, Geuze HJ, Stoorvogel W 2003 Proteomic and biochemical analyses of human B cell-derived exosomes. Potential implications for their function and multivesicular body formation. *J Biol Chem* 278:10963–10972
46. Furukawa S, Fujita T, Shimabukuro M, Iwaki M, Yamada Y, Nakajima Y, Nakayama O, Makishima M, Matsuda M, Shimomura I 2004 Increased oxidative stress in obesity and its impact on metabolic syndrome. *J Clin Invest* 114:1752–1761
47. Tang HY, Ali-Khan N, Echan LA, Levenkova N, Rux JJ, Speicher DW 2005 A novel four-dimensional strategy combining protein and peptide separation methods enables detection of low-abundance proteins in human plasma and serum proteomes. *Proteomics* 5:3329–3342
48. Hausman GJ, Richardson RL 1983 Cellular and vascular development in immature rat adipose tissue. *J Lipid Res* 24:522–532
49. James G, Olson EN 1990 Fatty acylated proteins as components of intracellular signaling pathways. *Biochemistry* 29:2623–2634
50. Pajvani UB, Du X, Combs TP, Berg AH, Rajala MW, Schulthess T, Engel J, Brownlee M, Scherer PE 2003 Structure-function studies of the adipocyte-secreted hormone Acrp30/adiponectin. Implications for metabolic regulation and bioactivity. *J Biol Chem* 278:9073–9085
51. Stoorvogel W, Kleijmeer MJ, Geuze HJ, Raposo G 2002 The biogenesis and functions of exosomes. *Traffic* 3:321–330
52. Fevrier B, Raposo G 2004 Exosomes: endosomal-derived vesicles shipping extracellular messages. *Curr Opin Cell Biol* 16:415–421
53. Stubbs JD, Lekutis C, Singer KL, Bui A, Yuzuki D, Srinivasan U, Parry G 1990 cDNA cloning of a mouse mammary epithelial cell surface protein reveals the existence of epidermal growth factor-like domains linked to factor VIII-like sequences. *Proc Natl Acad Sci USA* 87:8417–8421
54. Shojima N, Sakoda H, Ogihara T, Fujishiro M, Katagiri H, Anai M, Onishi Y, Ono H, Inukai K, Abe M, Fukushima Y, Kikuchi M, Oka Y, Asano T 2002 Humoral regulation of resistin expression in 3T3-L1 and mouse adipose cells. *Diabetes* 51:1737–1744
55. Wu X, Zhu L, Zilbering A, Mahadev K, Motoshima H, Yao J, Goldstein BJ 2005 Hyperglycemia potentiates H₂O₂ production in adipocytes and enhances insulin signal transduction: potential role for oxidative inhibition of thiol-sensitive protein-tyrosine phosphatases. *Antioxid Redox Signal* 7:526–537
56. Greco V, Hannus M, Eaton S 2001 Argosomes: a potential vehicle for the spread of morphogens through epithelia. *Cell* 106:633–645
57. Vincent JP, Magee T 2002 Argosomes: membrane fragments on the run. *Trends Cell Biol* 12:57–60
58. Wang W, Kirsch T 2002 Retinoic acid stimulates annexin-mediated growth plate chondrocyte mineralization. *J Cell Biol* 157:1061–1069
59. Wu LN, Genge BR, Kang MW, Arsenault AL, Wuthier RE 2002 Changes in phospholipid extractability and composition accompany mineralization of chicken growth plate cartilage matrix vesicles. *J Biol Chem* 277:5126–5133
60. Heijnen HF, Schiel AE, Fijnheer R, Geuze HJ, Sixma JJ 1999 Activated platelets release two types of membrane vesicles: microvesicles by surface shedding and exosomes derived from exocytosis of multivesicular bodies and α -granules. *Blood* 94:3791–3799
61. Satta N, Toti F, Feugeas O, Bohbot A, Dachary-Prigent J, Eschwege V, Hedman H, Freyssinet JM 1994 Monocyte vesiculation is a possible mechanism for dissemination of membrane-associated procoagulant activities and adhesion molecules after stimulation by lipopolysaccharide. *J Immunol* 153:3245–3255
62. Thery C, Zitvogel L, Amigorena S 2002 Exosomes: composition, biogenesis and function. *Nat Rev Immunol* 2:569–579
63. Dolo V, Li R, Dillinger M, Flati S, Manela J, Taylor BJ, Pavan A, Ladisch S 2000 Enrichment and localization of ganglioside G(D3) and caveolin-1 in shed tumor cell membrane vesicles. *Biochim Biophys Acta* 1486:265–274
64. Kim CW, Lee HM, Lee TH, Kang C, Kleinman HK, Gho YS 2002 Extracellular membrane vesicles from tumor cells promote angiogenesis via sphingomyelin. *Cancer Res* 62:6312–6317
65. Tarabozetti G, D'Ascenzo S, Borsotti P, Giavazzi R, Pavan A, Dolo V 2002 Shedding of the matrix metalloproteinases MMP-2, MMP-9, and MT1-MMP as membrane vesicle-associated components by endothelial cells. *Am J Pathol* 160:673–680
66. Gutwein P, Oleszewski M, Mechttersheimer S, Agmon-Levin N, Krauss K, Altevogt P 2000 Role of Src kinases in the ADAM-mediated release of L1 adhesion molecule from human tumor cells. *J Biol Chem* 275:15490–15497
67. Okamoto Y, Arita Y, Nishida M, Muraguchi M, Ouchi N, Takahashi M, Igura T, Inui Y, Kihara S, Nakamura T, Yamashita S, Miyagawa J, Funahashi T, Matsuzawa Y 2000 An adipocyte-derived plasma protein, adiponectin, adheres to injured vascular walls. *Horm Metab Res* 32:47–50
68. Chavey C, Mari B, Monthouel MN, Bonnafous S, Anglard P, Van Obberghen E, Tartare-Deckert S 2003 Matrix metalloproteinases are differentially expressed in adipose tissue during obesity and modulate adipocyte differentiation. *J Biol Chem* 278:11888–11896